



**EFFECTIVENESS OF THE MAIN RING ABORT DUMP**

W. Lee and J. A. MacLachlan

July 10, 1970

**A. INTRODUCTION**

The main ring abort system as currently conceived<sup>1</sup> consists of a large block of material placed in long straight section E. Four full aperture vertical bump magnets provide an orbit kink to steer the beam into the block. This system with parameters appropriate to 500 BeV operation is shown in Figure 1. Because a significant fraction of the beam hits the dump at small angles, the scattering properties of the dump material strongly affect abort efficiency. This note describes Monte Carlo calculations of the effectiveness of various dumps in stopping primary beam particles. Several dump materials, a range of beam conditions, and varying dump geometry have been considered. The paths of the protons in the dump are calculated by the computer subroutine MONACO<sup>2</sup> which includes nuclear and multiple coulomb scattering (MCS). The development of the nuclear cascade is not followed; however, results from the Monte Carlo programs TRANSK<sup>3</sup> and FLUTRA<sup>4</sup> are used to estimate results of the cascade.

**B. COMPUTATIONAL PROCEDURE**

The dump efficiency is found by following several thousand



particles from a uniformly bright beam ellipse one-by-one. The subroutine MONACO<sup>2</sup> which calculates particle trajectories through material has been modified to permit a piecewise straight edge for studying effects of dump shape. The effect of the beam bump is represented by sweeping the beam ellipse onto the dump in twelve equal steps; thus, the calculation considers what happens to that part of the beam which hits the dump as the beam is being swept on to the up stream end of the dump. For each step the kick angle is different; particle incident angles are the sum of their phase space angular coordinate and the current kick angle. When the kick is sufficient that all of the beam hits end on, the primary stopping efficiency is nearly 100%. To get the efficiency for the entire dump process, one multiplies the program result by the ratio  $\frac{\theta_f - \theta_i}{5 \cdot 10^4 \omega_k}$ , where  $\theta_i$  is kick angle at first incidence,  $\theta_f$  is kick angle for all beam hitting the end,  $\omega_k$  is kick angle per turn, and  $5 \cdot 10^4$  is the number of particles followed by the program. Thus, efficiency is the ratio of a figure of merit for the dump to the bump rate. A flow diagram of the program is given in Figure 2. The free parameters are the dump material, the beam momentum, beam emittance, and dump shape.

### C. DISCUSSION OF RESULTS

The relative merit of any particular set of dump parameters must be judged in terms of its primary stopping

efficiency, the angular distribution of the scattered beam, the cascade trapping efficiency, the thermal load tolerance, and economy. The choice of the dump material is relevant to all of these properties.

The behavior of the dump for primary particles may be crudely approximated by a uniform parallel beam hitting the dump block end on. Table I gives the out scattered fraction  $F$  (%) and average scattered angle  $\theta$  (mrad) of a beam 1 cm high normally incident at the bottom edge of a block for several materials according to MONACO, according to MONACO with MCS only, and according to a simplified MCS calculation by Lee Teng<sup>1</sup>. One can see that the multiple coulomb result is a good guide, particularly for the heavy elements because of the  $Z^2$  dependence of the radiation length. For the lighter elements, however, nuclear scattering causes about half of the particle loss. All of the materials tried lie within about a factor of two in effectiveness. Aluminum and lead stand out as particularly bad because of low density for their atomic weights. Iron looks nearly as good as tungsten and is much cheaper and easier to work.

The basic goal in the choice of a dump geometry is that little beam hits the dump at grazing angles. Thus, the bulk of material should be parallel to the bumped orbit. The bump angle at which the beam first hits is, however, a function of beam width and thus of beam momentum and machine conditions. If the beam has blown up to full aperture, a substantial

fraction hits on the lowest part of the dump. To have good stopping efficiency for this part of the beam several interaction lengths should back up the lowest point. Therefore, it is not satisfactory to tip a flat block at some nominal bump angle. For a wide beam the initial bump angle is zero and the first part of the block should be aligned parallel to the unperturbed orbit. (See Figure 3.) The length of this piece depends on the material and a trade off between primary and secondary stopping efficiencies.

The length  $\ell_1$  determines the percentage of the beam hitting the bottom face of the dump, but as Table II shows the fraction escaping does not go up proportionately at 200 BeV. For lower incident energy the fraction escaping is more sensitive to the fraction hitting the bottom, because the multiple scattering angle becomes comparable to the incidence angle and leakage occurs from the entire bottom surface, not just the downstream end. A value of 1 m was assigned to  $\ell_1$  in the optimization of the tilt of  $\ell_2$  although this value can be shorter for an iron dump. The total length of the dump is determined by the need for near total absorption. M. Awschalom<sup>5</sup> has suggested that about 6 m of iron should suffice.

Primary stopping efficiency is plotted in Figure 4 of 6 m iron dumps vs. tilt angle of the last 5 m with beams of 8, 200, and 500 BeV at both design emittance and full aperture. These abscissa values refer to a bump rate of 4 cm/turn at 500 BeV; they can be linearly scaled to any other reasonable

rate. The curves are labeled by the beam energy and "N" for a nominal design emittance beam and "W" for a full aperture beam. Other results of our calculation include the angular distribution of the outscattered primaries and the longitudinal distribution of the primary stars. The approximate correlation of the momentum dependence of bump rate and scattering angles can be seen from the close proximity of the curves. Furthermore, one can infer an optimum tilt angle of about 1.5 to 2 mrad for the downstream length  $\ell_2$ .

Having established an improved geometry we return to a selection of materials to check that more realistic beam conditions do not affect the earlier conclusions. Table III gives escape percentages for a design emittance 200 BeV beam incident on dumps of several materials. The differences from the divergenceless beam example given in Table I are noticeable, but materials rank in the same order except for the breaking of the tie between lead and aluminum. Iron seems to remain the practical choice.

It has been suggested<sup>6,7</sup>, particularly in connection with scrapers, that it is advantageous to have a surface which is hit at small angles faced with a low Z material. This suggestion is not important for this dump design because most protons are incident at angles greater than those characterizing MCS. Therefore, the average nuclear scattering angle and the interaction length are more sensitive parameters.

Unfortunately, short nuclear interaction length and short

radiation length go together so that the most efficient dump for primaries also concentrates the energy deposition the most. Shoemaker<sup>8</sup> suggests that reliable operation of the magnets is more likely for a bump rate 1 cm/turn or less. Assuming this rate one has for a very thin beam an effective height of 1 cm and a width of  $w_x = \sqrt{\epsilon_x \beta_x}$ . The nuclear and electromagnetic cascade program FLUTRA<sup>4</sup> has been run for a 400 BeV beam 1 cm x 1 cm incident on the axis of a 6 m long iron cylinder. The transversely integrated energy deposition agrees to better than 20% with calorimeter curves obtained by Jones et. al.<sup>9</sup> with muons. According to FLUTRA the energy deposition per incident proton reaches a peak of  $3.7 \times 10^{-10}$  cal/cm<sup>3</sup> along the beam axis about 30 cm into the iron. One cal/cm<sup>3</sup> gives about 1° C temperature rise in iron; thus a flux less than  $4 \times 10^{12}$  protons at 400 GeV will not melt an iron dump. Although this result is only indicative because the beam width is not correctly handled and because the real dump will lose cascade products through the bottom face, it appears that steel is unsuited to design intensity at 400 BeV. In this respect aluminum is far superior. The FLUTRA result for peak temperature rise is about  $2 \times 10^{-11}$  °C/proton at about 85 cm into the block. Therefore, if the dump is configured as shown in Figure 3, the temperature will be about melting for  $5 \cdot 10^{13}$  protons/pulse at 400 BeV. The 10 cm thickness of the aluminum insert is chosen from the radial distribution of energy deposition in the FLUTRA aluminum run which shows the flux down more than one hundred

fold 10 cm from the beam axis at the depth of peak deposition. The length of  $2\frac{1}{2}$  meters is chosen to reduce the energy deposition to less than one tenth of its peak value. The wider aperture iron extending upstream from the aluminum has been suggested by M. Awschalom<sup>5</sup> to catch backward production. It would be prudent to instrument the dump with a few thermocouples. In view of the uncertainties in both the Monte Carlo calculation and the cosmic ray observations which roughly validate it, the suggested dump could well be adequate even for full intensity at 500 BeV. The step from 400 to 500 is sufficiently small so that according to Jones' curves the peak energy deposition is obtained by linear extrapolation. This 25% effect is smaller than a reasonable uncertainty estimate for the calculation.

#### Acknowledgements

We gratefully acknowledge numerous discussions of this material with Miguel Awschalom, Frank Shoemaker and Lee Teng. The FLUTRA runs and extensive help in their interpretation were provided by Tom Borak.

References

1. L. C. Teng, NAL, FN-195 (1969).
2. J. MacLachlan, T. Borak, and M. Awschalom, NAL, TM-244 (1970).
3. J. Ranft, Improved Monte Carlo Calculation of the Nucleon-Meson Cascade in Shielding Materials, CERN/MPS/Int. MU/EP 66-8 (1966).
4. J. Ranft, private communication.
5. M. Awschalom, private communication.
6. J. Ranft, RHEL NIMROD (BP) 69-4.
7. F. C. Shoemaker, NAL, TM-188 (1969).
8. F. C. Shoemaker, NAL, TM-255 (1970).
9. L. W. Jones, et. al., unpublished.



TABLE I  
Outscattered Fraction F of 1 cm High Uniform  
Beam and Average Scattered Angle  $\bar{\theta}$

<u>Material</u>	MONACO		MONACO (Multiple Coulomb Only)		Analytic <sup>(1)</sup> (Multiple Coulomb Only)	
	<u>F(%)</u>	<u><math>\bar{\theta}</math> (mrad)</u>	<u>F(%)</u>	<u><math>\bar{\theta}</math></u>	<u>F(%)</u>	<u><math>\bar{\theta}</math> (mrad)</u>
B <sub>e</sub>	.28	.91	.07	.10	.11	.087
Al	.34	.72	.19	.24	.20	.17
F <sub>e</sub>	.22	.70	.15	.39	.13	.25
C <sub>u</sub>	.22	.79	.14	.44	.13	.27
W	.18	.94	.17	.75	.14	.44
P <sub>b</sub>	.36	1.0	.35	.80	.27	.46
U	.25	1.0	.21	.87	.18	.49

TABLE II  
Comparison of Dump Shape

Dump Shape:  $\phi = 2$  mrad  
Beam Momentum: 200 BeV/c  
Beam Emittance: N...0.09  $\pi$ mm mrad  
W...4.555  $\pi$ mm mrad

<u><math>l_1, l_2</math> (m)</u>	<u>Emittance</u>	<u>% of The Beam Escaped</u>	<u>% of The Beam Hit The Bottom of The Dump</u>	<u><math>\theta</math> of Escaped Beam (mrad)</u>
0.5,5.5	N	0.1003	0.986	1.124
1.0,5.0	N	0.1007	1.898	1.05
6.0,0.0	N	0.2016	8.594	0.757
0.5,5.5	W	0.091	1.358	1.079
1.0,5.0	W	0.115	2.14	1.093
6.0,0.0	W	0.239	8.386	1.303

TABLE III  
Comparison of Dump MaterialsDump Shape  $\ell_1 = 1 \text{ m}, \ell_2 = 5 \text{ m}, \phi = 2 \text{ mrad}$ 

Beam Momentum: 200 BeV/c

Beam Emittance: 0.09 mm mrad

<u>Material</u>	<u>% of The Beam Escaped</u>	<u><math>\theta</math> of Escaped Beam (mrad)</u>
Be	0.225	1.1765
C ( $\rho=2.25$ )	0.195	1.1068
Al	0.248	1.0991
Fe	0.101	1.05
Cu	0.093	0.9801
W	0.067	0.8108
Pb	0.121	0.9025
U	0.077	0.7904

Figure 1: Abort System

stopper

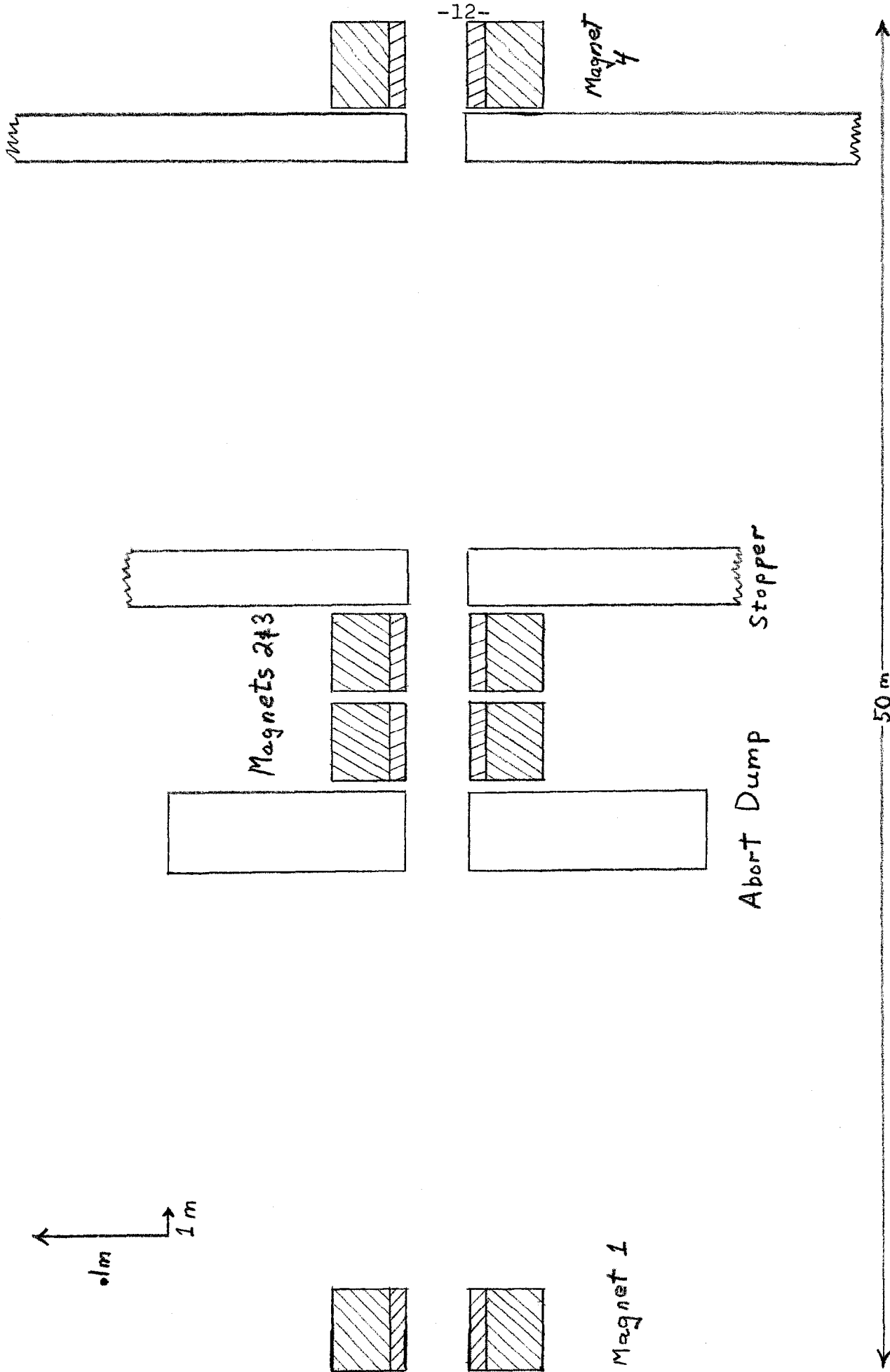
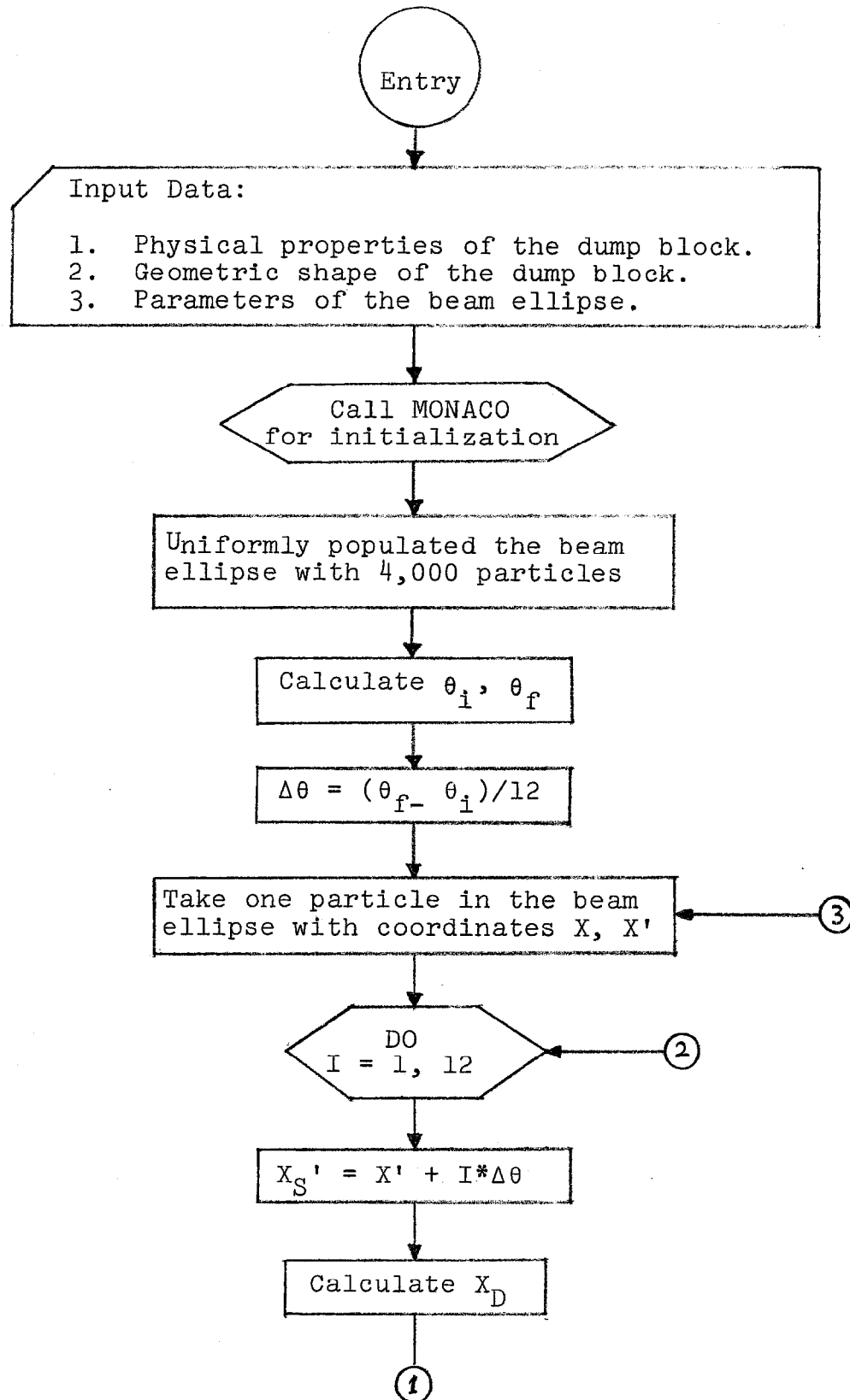
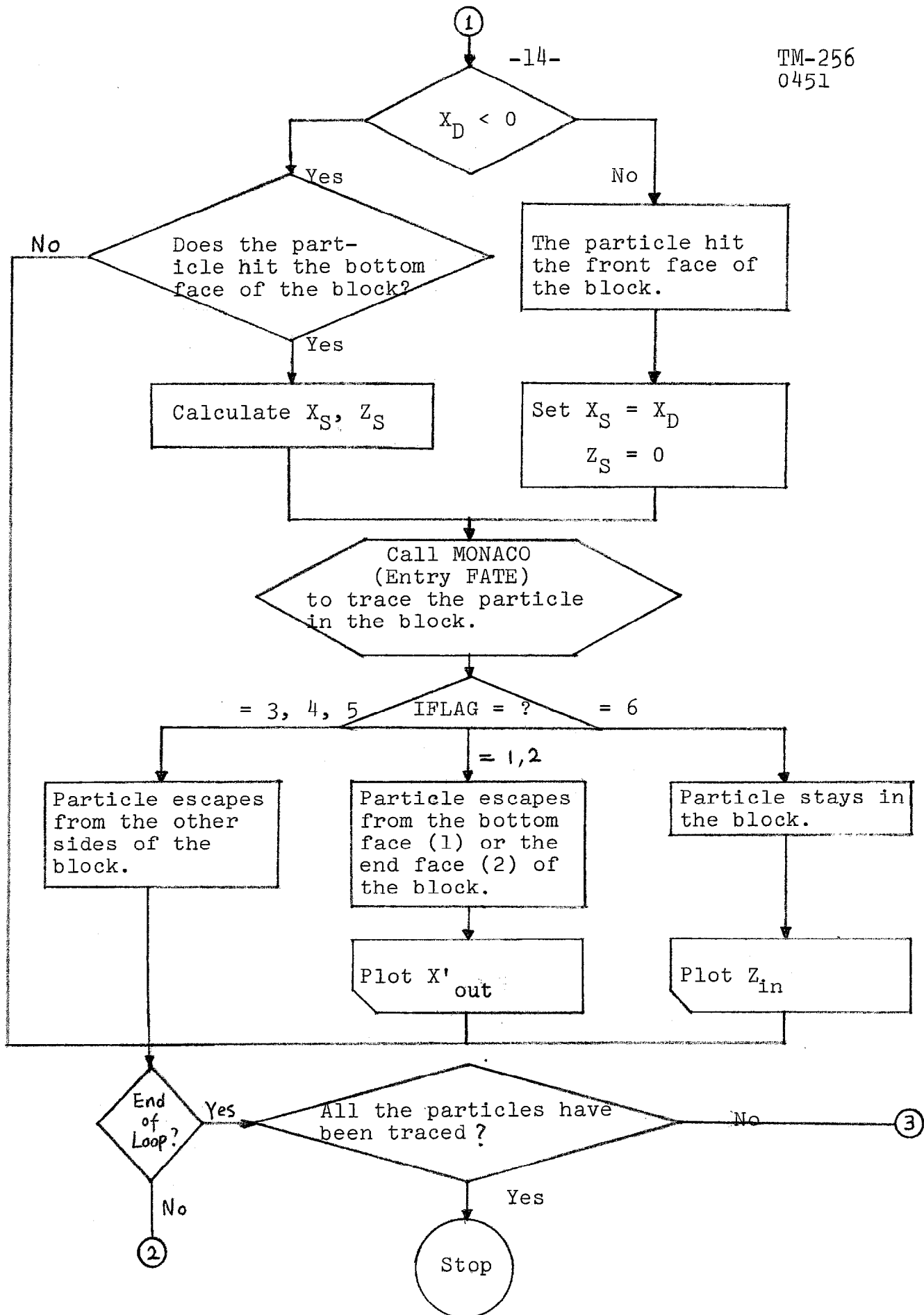


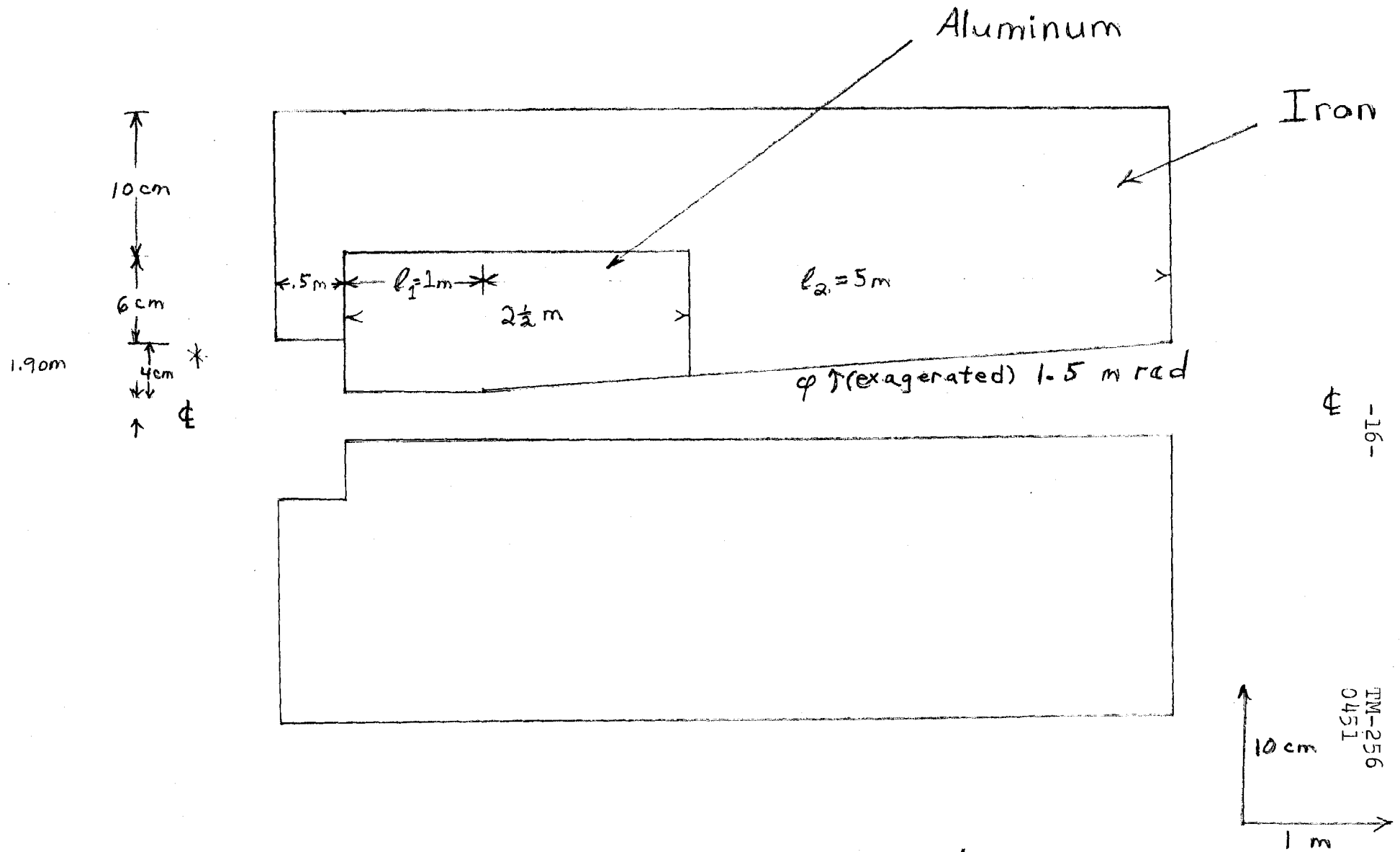
Fig. 2 Flow Diagram of the Program





$\theta_i$	the kick angle corresponding to the initial contact of the beam ellipse with the dump block
$\theta_f$	the kick angle when all the beam ellipse has hit the front face of the block
$\Delta\theta$	increment of the kick angle
$X, X'$	transverse phase space coordinates of the particle in the beam ellipse
$X_D$	the vertical distance of the particle from the lower edge of the block when the particle reaches the front face
$X_S, Z_S$	the vertical and horizontal position of the particle when it hits the block
$X'_{out}$	scattering angle of the particle which escapes from the block
$Z_{in}$	the longitudinal position in the block of a nonelastic event

Figure 3: Longitudinal Section of Abort Dump



\* Adjust to equal per turn beam displacement used



N: beam with design emittance

W: full aperture beam

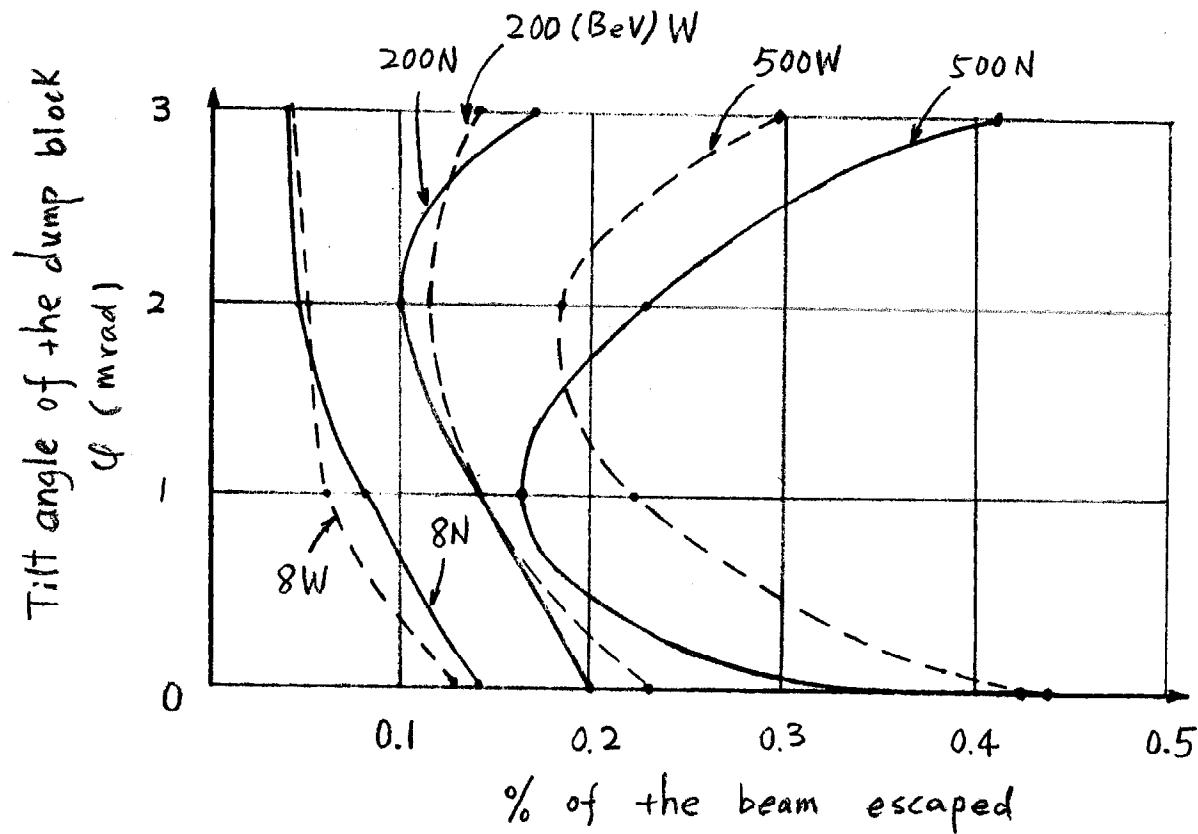


Fig. 4 Effectiveness of the dump block with  $l_1 = 1\text{m}$  and  $l_2 = 5\text{m}$  vs. tilt angle  $\phi$  for beams of various momenta